Single-pixel thermopile infrared sensing for people counting

Erik Hagenaars[1], Ashish Pandharipande[1], Abhishek Murthy[2], Geert Leus[3]

***Abstract*— People-counting data can be used in building-control systems to improve comfort and in space management applications to optimize building space. In this work, we consider a combi-sensor with a single-pixel thermopile and passive infrared sensor for people counting. We first develop a thermopile signal model for object temperature measurements under multiple people occupancy. We then propose a people counting method based on: cumulative sum (CUSUM) change detection in the object temperature signal, forming a people count estimate using likelihoods of differential mean temperature in detected changes, and decision fusion with an infrared vacancy sensor. The proposed method is evaluated with data generated using the developed signal model as well as experimental data from a cell office/meeting room environment. We obtain an average counting error of 0.11 and 0.19 for 90% of the instants respectively when considering 15 minute windows for simulated and experimental datasets.**

***Index Terms*— Single pixel thermopile sensor, infrared sensing, people counting, temperature model, change detection.**

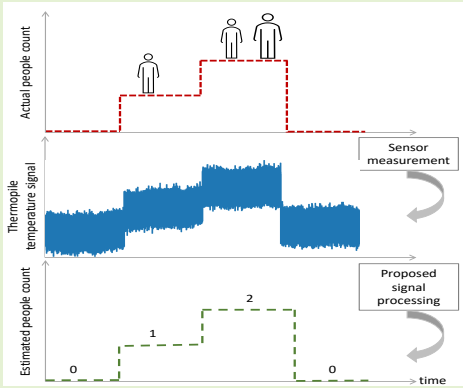

I. Introduction

People count in an indoor space is the amount of users dwelling in that space. In office buildings, people count data can be used in smart lighting and HVAC (Heating, Ventilation and Air Conditioning) control systems to improve user comfort, and in space management applications to improve utilization of workspaces. The amount of heating, cooling and air circulation may be adapted in HVAC control systems based on the amount of people in an area [1], thus providing higher levels of comfort to users while optimizing energy consumption based on spatio-temporal people count patterns [2], [3]. Space management applications like space portfolio management and workspace recommendation use people counting data with the objective of achieving higher utilization of building space in a way that matches user and business needs [4]–[7]. Historical people counting data may be used to identify area of low utilization, assess the existing building space portfolio and then tailor it to evolving usage patterns and future space needs. In workspace recommendation applications, people counting data is used to assist users in real time to find available workspaces in a flexible workplace environment.

[1] The authors are with Signify, High Tech Campus, Eindhoven, The Netherlands. Email: {erik.hagenaars, ashish.p}@signify.com
[2] The author is with Signify, Cambridge, USA. Email: abhishek.murthy@signify.com
[3] The author is with Delft University of Technology, Delft, The Netherlands. Email: g.j.t.leus@tudelft.nl

A. Our approach to people counting and contributions

We consider a thermopile infrared sensing solution for people counting. We use a combi-sensor with a single-pixel thermopile sensor and a passive infrared (PIR) sensor. Individually, these sensors are used respectively for remote temperature measurements (used for HVAC control applications) and occupancy based controls (e.g. turning on/off lighting in an area). In our approach, we consider these sensor modalities in combination for people counting. A single-pixel thermopile sensor measures the radiated infrared temperature of objects. Multiple challenges need to be addressed to estimate people count using these measurements. One, the background temperature is affected by ambient effects like HVAC activation or air drafts. Two, the measured temperature depends on object characteristics like position and orientation of users with respect to the sensor. Three, the impact of a user entering an area on the temperature measurement differs from the user leaving the area.

To address these challenges, we consider the following approach. A CUSUM-based change detector is applied to a recursive least squares (RLS) estimate of the temperature signal to detect abrupt changes, associated with a change in people count in an area, in the slowly varying temperature signal. A differential mean temperature between change points is computed and then mapped to a people count estimate using a likelihood approach. Finally, a decision fusion of the people count estimate with vacancy detection from the PIR sensor is used to determine vacancy.

To facilitate performance analysis of our approach, we

develop an analytical model of the thermopile sensor signal under people occupancy. The model allows us to evaluate the performance with respect to several parameters: noise levels, temperature changes under people occupancy and temperature transition speed. Using both simulation data and experimental data from cell office and meeting room setups, we achieve an average counting error of 0.11 (0.19) and 0.19 (0.25) for 90% of instants respectively when considering 15 minute (1 minute) windows for simulated and experimental datasets.

In Section II, we describe the thermopile signal model. The proposed sensor signal processing steps are described in Section III. In Section IV, simulation and experimental results evaluating people counting estimation are presented. We conclude in Section V.

B. Past approaches to people counting

Different approaches to people counting in indoor environments have been studied in the past. We shall briefly discuss only the non-intrusive approaches; thus approaches where users carry tags or use badges are not discussed. Image sensors [8]–[11] can provide people count estimates with high accuracy and have become cost-effective due to the proliferation of camera-based smartphones; however imaging modalities are perceived to be the most invasive on privacy and influence the behaviour of the affected people [12], [13]. Thermopile arrays [14]–[17] use thermal images for people counting. The accuracy is good and the sensors are less invasive, but array sensors are still quite expensive. Ultrasonic arrays [18], [19] and WiFi-based [20], [21] device-free passive approaches are the least invasive, but potentially have lower people counting accuracy.

Binary sensor networks, wherein each sensor (e.g. PIR) produces a binary detection, together with advanced fusion techniques have also been explored for people tracking and counting [22], [23]. An advantage of this solution is that the sensor infrastructure may be part of a pre-existing connected lighting system, and thus people counting can be done without the need of deploying extra hardware. A drawback of using PIR sensor networks is however that the accuracy of people counting is limited.

II. Thermopile Temperature Signal Model

A thermopile sensor provides the temperature of objects from a distance by detecting the combined object's infrared energy within its Field of View (FoV). This means that the thermopile sensor has a different object temperature output for different amounts of incident infrared energy, depending on factors like object positions and orientations. In Figure 1, the object temperature signal from a single-pixel thermopile sensor mounted at the ceiling is shown for varying occupancy levels. The temperature can be observed to gradually increase in the first hour, even under constant occupancy, due to the room temperature being controlled by the HVAC. It can also be observed that the mean object temperature under vacancy is not constant over time and depends on factors like HVAC control and occupancy levels prior to occupancy (e.g., the temperature decreases gradually when people count changes from 2 to 0 around 14:40).

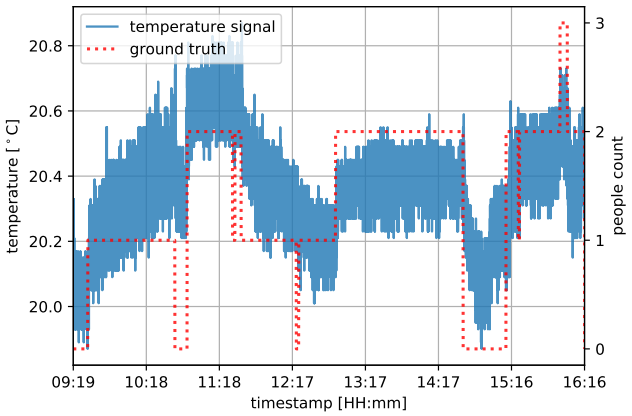

Fig. 1. Example of thermopile object temperature data starting at vacancy and ending in activity.

The signal model consists of three components: (i) signal component under vacancy, (ii) attenuation model due to sensor FoV, and (iii) signal component under presence of multiple people.

A. Signal under vacancy

During periods of vacancy, the temperature variations are typically slow and happen due to factors like daylight changes and HVAC control. We model the thermopile temperature signal over vacancy by a slowly varying value $T_0[n]$ with an additive noise component $v[n]$,

$$x[n] = T_0[n] + v[n]. \tag{1}$$

In Figure 2, we show object temperature data from three thermopile sensors over a 7 hour period under vacancy. The gradual temperature rise is on account of the HVAC system being disabled at night. The measured object temperature was tested for normality by testing the null hypothesis if the sample given comes from a normal distribution. The test combines the skew and kurtosis to test this property based on the D'Agostino-Pearson test [24], [25]. The normality test returns the probability that a null hypothesis can be rejected. When the null hypothesis rejection probability is lower than a threshold, a normal distribution can be assumed. We observed that $v[n]$ can be modeled as an additive white Gaussian noise (AWGN) component when considering a short duration of time. For a window of 9000 samples (15 min), and with a typical threshold value of 10^{-3}, 97% of the windows could be considered normally distributed.

B. Attenuation model due to sensor FoV

The thermopile sensor is not omni-directional, but rather has a limited FoV with variable signal attenuation. The signal amplitude under occupancy thus depends on the location of the object with respect to the center of the sensor. For instance, for the thermopile sensor component from Melexis [26] we use in our experiments, there is no attenuation when directly

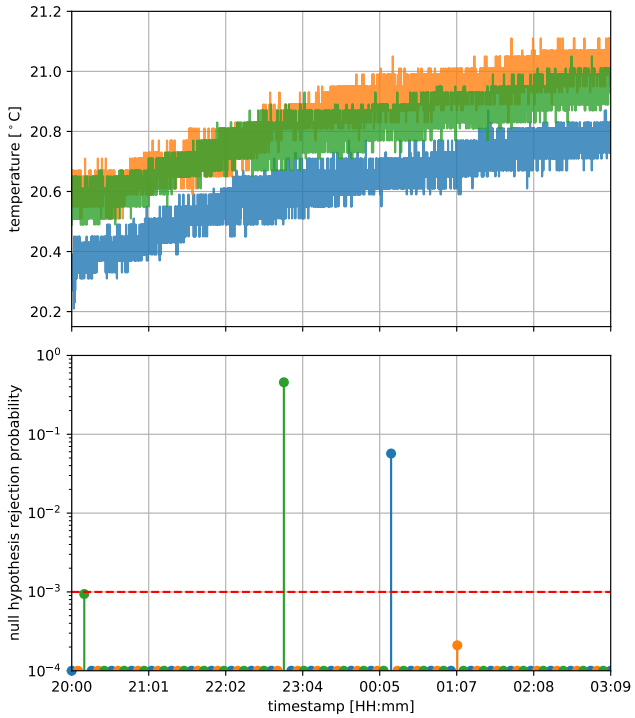

Fig. 2. Top: Temperature data of three sensors under vacancy. Bottom: Normality test for windows of 15 min (9000 samples).

under the sensor (around $0°$) and a 3 dB loss at an angle of $45°$.

We use a raised cosine function to model the attenuation due to sensor FoV,

$$f(\theta) = \begin{cases} 1 & \theta \leq \frac{1-\rho}{2T} \\ \frac{1}{2} + \frac{1}{2}\cos\left(\frac{\pi T}{\rho}\left[\theta - \frac{1-\rho}{2T}\right]\right) & \frac{1-\rho}{2T} < \theta \leq \frac{1+\rho}{2T} \\ 0 & \theta > \frac{1+\rho}{2T}, \end{cases} \quad (2)$$

where θ is the angle between the user and center of the sensor, and T and ρ are parameters. Parameter values $T = 1/90$ and $\rho = 0.4$ are chosen to have an attenuation function close to the FoV specifications of the chosen sensor [26]. Note that in the above model, we have ignored the impact of object distance from the sensor. In typical office applications, the sensor is installed at the ceiling at heights between 2.5-3.5 m, with the seated user/workspace 1-2.2 m away from the sensor. Within this distance range, the temperature measurements have negligible variation, and hence we have ignored range dependence. The resultant raised cosine function to model the FoV attenuation is shown in Figure 3.

C. Signal under presence of multiple people

The presence of one or more people produces a temperature shift in the object temperature value of the thermopile sensor. The shift depends on the number of people, their locations and secondary aspects like orientation. Furthermore, the shift in temperature value transitions faster during entry of people and slower when people leave, due to occupants having heated the environment and leaving a thermal footprint that fades with time.

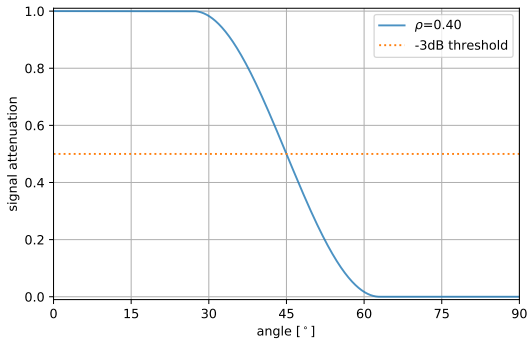

Fig. 3. Attenuation function due to limited sensor FoV.

We model these temperature shifts using an exponential model with parameters being the total temperature shift and the transition speed as follows

$$d_i[n] = \Delta T_i^o \left(1 - e^{-\alpha_i(n-n_i)}\right) u[n - n_i]. \quad (3)$$

The parameter ΔT_i^o is the temperature shift for event i at time sample n_i and $u[n]$ is the unit step function. Parameter α_i captures transition speed of temperature change due to an occupancy event, and has a bigger value for an entry event and a smaller value for an exit event.

D. Thermopile signal model

Putting together the earlier signal components, we can now write the thermopile signal model for K_m events preceded by initial vacancy as

$$x[n] = T_0[n] + v[n] + \sum_{i=1}^{K_m}\sum_{j=1}^{K_i} f(\theta_{ij}) d_{ij}[n]. \quad (4)$$

In (4), till time sample n_1, there is vacancy and the temperature is at an initial temperature T_0 with AWGN $v[n]$. At time sample n_i, we consider K_i occupants with the j-th occupant at angle θ_{ij} with respect to the sensor resulting in temperature shift d_{ij}. At event i, there is an *effective temperature change* of ΔT_i (taking into account users located at different angles).

A simulated example of the dataset using the model in (4) with 10 occupancy events is shown in Figure 4. The ground truth with actual people count is shown in dotted red line.

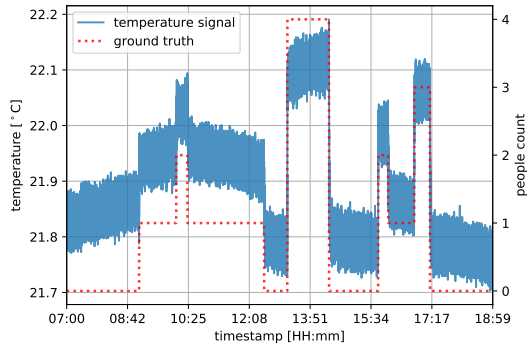

Fig. 4. Example of a simulated dataset over a day.

III. Sensor signal processing

The various sensor signal processing blocks for people counting are depicted in Figure 5. The thermopile object temperature signal is pre-filtered to remove any outlier data. This signal is then used to detect sudden changes in temperature levels. The mean temperature change between change points is then determined and a maximum likelihood estimate of people count is obtained. The people count estimate is fused with the vacancy detection output of the PIR sensor to obtain a final people count estimate.

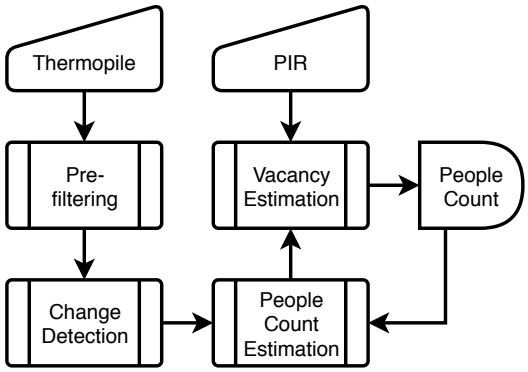

Fig. 5. Overview of sensor signal processing blocks.

A. Pre-filtering

The first step in processing the thermopile object temperature data is to remove outliers, that may arise due to electrical noise sources. A simple inter-quartile filter is used to remove large outlier values. We calculate the z-score of every sample in a window,

$$z[n] = \frac{x[n] - \hat{\mu}}{\hat{\sigma}} \tag{5}$$

where $\hat{\mu}$ and $\hat{\sigma}$ are the sample mean and standard deviation of values within the window. If the z-score exceeds a certain threshold, the sample is removed. Denote the signal obtained subsequent to this filtering by $y[n]$.

B. Change detection using CUSUM RLS

After the pre-filtering step, change points are detected in signal $y[n]$. An important feature to detect a change in people count is the resulting change in temperature level. To detect sudden changes in a slowly varying signal with minimal knowledge of the signal, we adopt the CUSUM RLS change point detection proposed in [27]. Here a change point is detected when the cumulative sum of the difference between the RLS estimate of the signal and the actual value exceeds a certain threshold. Denote the RLS estimate of signal $y[n]$ by

$$\hat{T}[n] = \beta\hat{T}[n-1] + (1-\beta)y[n], \tag{6}$$

where $0 < \beta < 1$ is a forgetting factor. At a sudden change $n = k$ and some samples beyond, the error term

$$\epsilon[n] = y[n] - \hat{T}[n] \tag{7}$$

will be large since the RLS estimation will introduce a delay in the estimate's response. If this transition is not sudden but gradual, the cumulative sum of these terms

$$g_p[n] = \max\left[g_p[n-1] + \epsilon[n] - \nu, 0\right] \tag{8}$$

$$g_m[n] = \min\left[g_m[n-1] + \epsilon[n] + \nu, 0\right] \tag{9}$$

will add up to become big. In (8) and (9), g_p and g_m respectively represent the cumulative sum of either the positive or negative changes. If the CUSUM surpasses a certain threshold, a change will be detected. A drift parameter, ν, is used to suppress noise in the CUSUM. An important design consideration lies in the selection of the forgetting factor β, the drift parameter ν and the threshold h. According to [27], the drift should be chosen such that at least 50% of the score is zero, while the forgetting factor should be chosen based on the maximum latency of the algorithm. Finally, the detection threshold is tuned to minimize the missed change event detections.

The traditional CUSUM resets the score when it surpasses a threshold. If the CUSUM would not reset the score g_m and g_p, the drift would force the score to approach 0 over time when the RLS estimate has settled to the new temperature level. At this sample, a new estimate of the mean is obtained from the RLS estimate.

C. People count estimation

We have two points of interest in the CUSUM score when one of the CUSUM signals (g_p or g_m) exceeds threshold h at sample n_p: (i) the last encountered zero index (n_l) in the score that exceeded the threshold and (ii) the first next zero index (n_r) encountered in the score that exceeded the threshold. The first zero index corresponds to the start of the temperature change. The CUSUM score continues to be calculated until it encounters the next zero index, when the RLS estimate has settled to the new temperature level:

$$g = \begin{cases} g_p, & \text{if } g_p[n_p] > h \\ g_m, & \text{if } g_m[n_p] < -h \end{cases} \tag{10}$$

with

$$n_l = i, \text{ when } g[i] = 0, g[j] \neq 0 \text{ for } i < j < n_p, \tag{11}$$

$$n_r = i, \text{ when } g[i] = 0, g[j] \neq 0 \text{ for } n_p < j < i. \tag{12}$$

Here, n_l and n_r denote the start and end respectively of the transition and the settling point of the RLS estimate to the new temperature level and g is either g_p or g_m depending on which of the scores exceeded the threshold. Calculating the difference of the RLS estimate at these points gives the estimation of the mean temperature change:

$$\Delta\hat{T} = \hat{T}[n_r] - \hat{T}[n_l]. \tag{13}$$

The output of the algorithm on the example dataset considered in Figure 4 is shown in Figure 6.

The temperature differential in (13) is then used to estimate the people count. This temperature change is dependent on

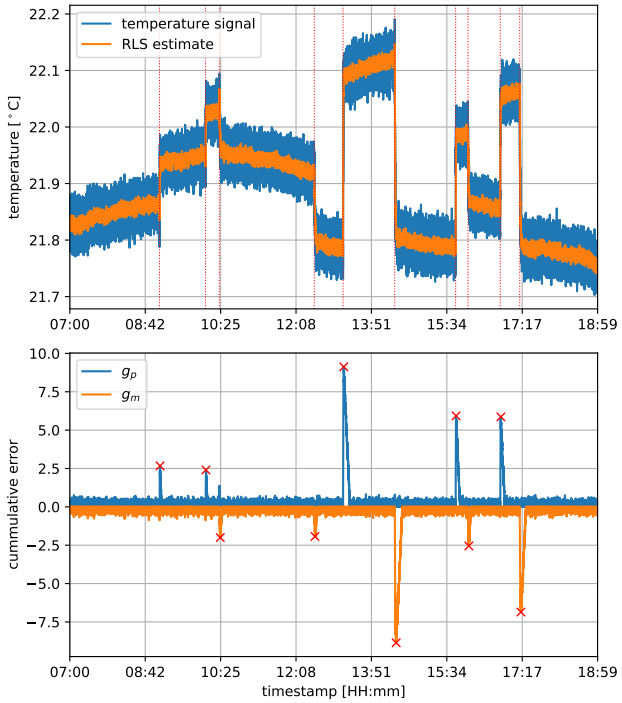

Fig. 6. Example of CUSUM RLS processing.

various factors: the number of people leaving or entering the room, the position at which the person(s) are located in the FoV, and the previous number of people in the FoV.

For every possible transition for a changing people count, we measure the temperature difference observed during that transition. From these measurements, a probability distribution of the temperature differential under various people count states is constructed. In Figure 7, we show the kernel density estimate with a Gaussian kernel for a sensor over an area with a maximum of 2 people. The three people count states ($p = 0$, $p = 1$ and $p = 2$) have two possible transitions each for which the estimated densities using an experimental dataset are shown. In general, for an area covered by a sensor with capacity of C people, we would have C states and a total of $C(C-1)$ probability distributions.

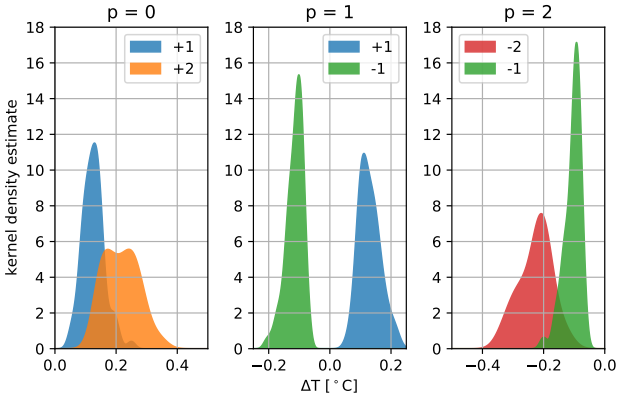

Fig. 7. Kernel density estimates of effective temperature change.

The people count estimation algorithm works as follows. For the current estimated people count, we consider the corresponding distributions. When a change is detected, for temperature differential $\hat{\Delta T}$, compute the posterior probabilities $\mathcal{L}(c|p[n-1], \hat{\Delta T})$. We then estimate the change in the occupancy $\hat{c}[n]$ corresponding to the temperature change by choosing the change corresponding to the maximum posterior and update the people count as follows,

$$\hat{c}[n] = \arg\max_c \mathcal{L}(c|\hat{p}[n-1], \hat{\Delta T}), \tag{14}$$

$$\hat{p}[n] = \hat{p}[n-1] + \hat{c}[n]. \tag{15}$$

The posterior in (14) can be computed using the likelihoods shown in Fig. 7 and applying Bayes rule with uniform priors. Contextual information, about the time-of-day and doorways can be used to make the priors informative.

D. Vacancy estimation

One of the challenges with people counting with the thermopile sensor is slow variation of temperature under vacancy. Furthermore, the dependence of mean temperature differential on human orientation characteristics may lead to errors in people count estimation, and thus possible error propagation. On the other hand, the PIR sensor is typically configured to have low false alarms (at the expense of high missed detections) [28], i.e., it can detect vacancy reliably. Instead of using the raw signal of a typical PIR sensor, the processed signal that controls lighting with built-in delay will be used. We adopt the following decision rule to combine the people count estimate of the thermopile sensor with the PIR sensor,

$$\hat{p}[n] = \begin{cases} \hat{p}[n-1] + \hat{c}[n], & \text{if PIR occupancy} \\ (\hat{p}[n-1] + \hat{c}[n])r, & \text{PIR vacancy and } \hat{p}[n-1] \geq 0.1 \\ 0, & \text{otherwise} \end{cases} \tag{16}$$

with $0 < r < 1$ a decay factor when vacancy is determined, and where $\hat{c}$ is the estimated people count from the temperature differential. The result of (16) will be that the people count is gradually set to 0 when the processed PIR signal determines vacancy. Since the people count estimate with the decay factor will never be zero, we force it to zero when small enough as indicated in the second condition in (16).

IV. Performance Evaluation

We evaluate the proposed method through exhaustive simulations using the signal model in (4) and using experimental data. The sampling frequency of raw sensor data was 10 Hz. A threshold of 3 was used in the pre-filtering step. The influence of various model parameters on the performance of the method is evaluated in subsection IV-A. The experimental evaluation is done in a cell office/meeting room environment in subsection IV-B and characterizes the performance of the method in a realistic indoor office environment.

Consider the error over a window of M samples,

$$\epsilon_{kj} = p_{kj} - \hat{p}_{kj}, \quad j = 1, \cdots, M, \tag{17}$$

where p_{kj} and $\hat{p}_{kj}$ are respectively the true people count and the estimated people count at sample k in window j.

We consider an error metric by discarding a portion of the errors, specifically the largest and smallest errors. This choice is driven by application considerations - small latencies or errors do not matter (e.g. a workspace where a user is away for a few minutes' break need not be considered vacant). Define the trimmed average counting error as

$$\epsilon_k^{(M)} = \frac{1}{(1-2\delta)M} \sum_{j=\delta M}^{(1-\delta)M} \left|\epsilon_{k[j]}\right| \tag{18}$$

where $\epsilon_{k[j]}$ is the ordered sequence of error terms ϵ_{kj} within the k-th window. The average counting error (ACE) is then given by

$$ACE(M) = \frac{1}{K} \sum_{k=1}^{K} \epsilon_k^{(M)}. \tag{19}$$

For $M = 1$, ACE(1) is simply the point-wise counting error. For other values of M, (19) provides an average error with the largest and smallest δ fraction of values removed; in the performance evaluation to follow, we choose $\delta = 0.1$. For instance, ACE(600) gives the average counting error for windows of duration 1 minute ignoring a few errors within this window. Such a performance metric better captures requirements for space management applications where a people counting value needs to be delivered every few minutes.

A. Simulation results

We use the signal model in (4) under different occupancy patterns to generate simulated data to evaluate the impact of various model parameters on performance. Three parameters are of interest: (i) the effective temperature, ΔT_i, which depends on angle of object with respect to sensor, user orientation and the sensor height, (ii) the transition speed, α, of an event, and (iii) sensor noise level, under normality assumption.

The distribution of the effective temperature change ΔT_i values are used to characterize the distributions based on which likelihood probabilities are computed and people count estimation done as per (14). In Figure 8, we see the performance based on this temperature change. The example is given for a zero to one transition event with varying values of effective temperature change. If the effective temperature change increase is too small, then it is difficult to detect an increase in people count leading to possible underestimation, and if the effective temperature change is too large then an overestimation in people count is likely to occur. We thus observe that ACE first decreases with the effective temperature change and then again increases.

In Figure 9, we evaluate ACE over a range of transition speed, α, values. We see that ACE reduces for higher values of α. The transition speed determines how fast the temperature level increases or decreases under an occupancy event. A higher value of transition speed indicates that the temperature change under an occupancy event is faster. The transition speed affects the size of peaks in the score of CUSUM RLS processing. For slower transitions, the RLS has a smaller error with the current sample, resulting in smaller peaks. It was found that the performance for slower transitions could be

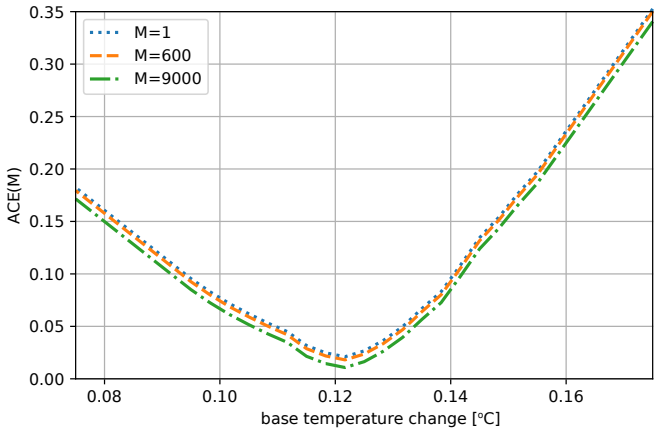

Fig. 8. ACE vs effective temperature change.

increased by increasing the forgetting factor. Another effect found when dealing with slower transitions was the increase in underestimating the mean temperature change since the score could prematurely converge to zero.

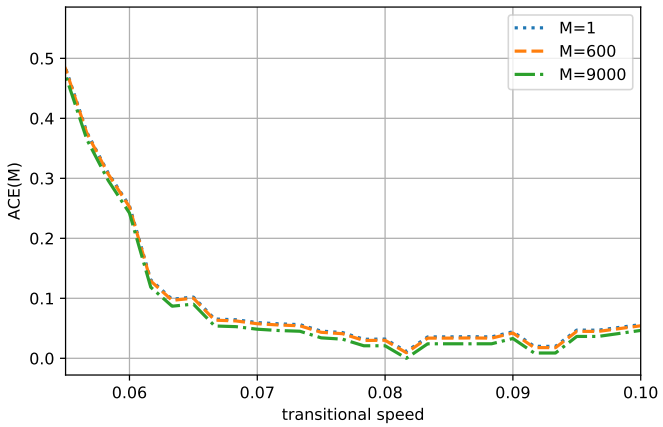

Fig. 9. ACE vs transition speed.

The noise levels which were encountered from real sensor data measurements were found to have minimal effect on the performance of the algorithm as can be seen in Figure 10. The ACE is lower for higher values of M; errors for $M = 1$ are largely due to the inherent latency of the algorithm.

People counting estimation results of the example simulation in Figure 4 for a single day is shown in Figure 11. In this case, it is observed that the people count estimate (green dashed line) matches with the ground truth (red dotted line) across all occupancy event scenarios.

Lastly, we show the cumulative distribution function (cdf) of ACE using simulated data in Figure 12. The range for the transition speed is used between 0.07 and 0.1 and the range of the effective temperature change is between 0.1 and 0.15. The noise level was chosen to be 0.05. From Figure 12, we see that with probability 0.9, ACE(1) = 0.23, ACE(600) = 0.19 and ACE(9000) = 0.11.

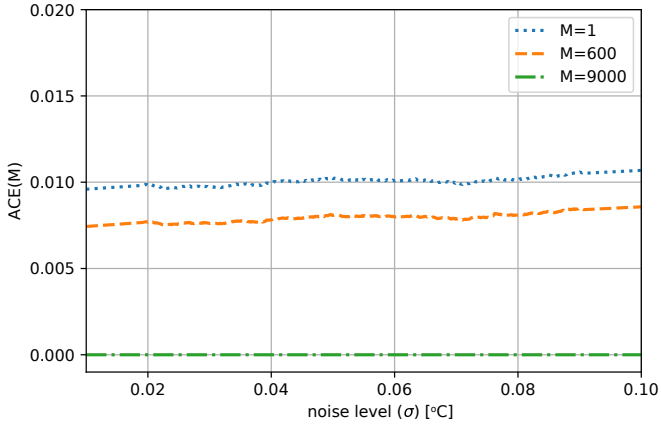

Fig. 10. ACE vs noise level.

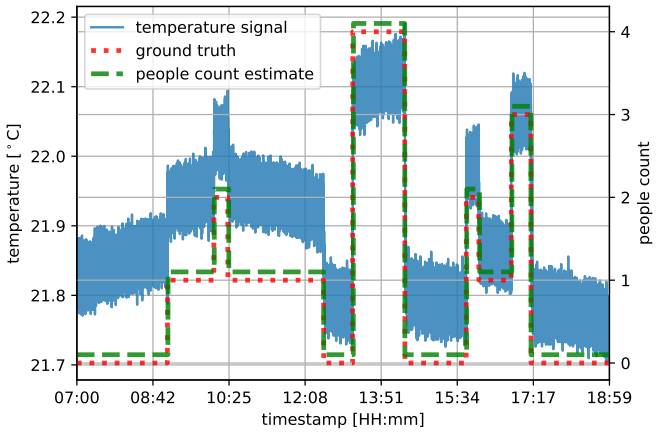

Fig. 11. Results of a simulated dataset.

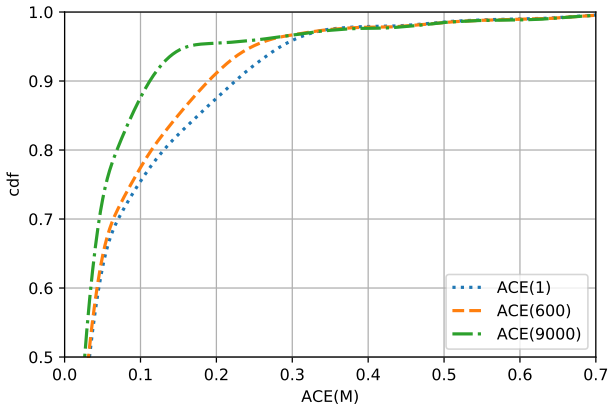

Fig. 12. Cumulative distribution for the results of the simulation for parameters in the range of the most common observed values.

Fig. 13. Experimental setup of indoor space with four workspaces, with a zoomed view of the sensor setup at the ceiling.

B. Experimental results

Experiments were conducted in a room emulating a cell office/ meeting room environment, with the setup shown in Figure 13. There were 4 combi-sensors at the ceiling at a height of 3.2 meter from the floor. There were 4 workspaces within the FoV of the sensors.

During measurements, occupancy events were recorded manually each day and served as the ground truth. Measurements were also collected overnight to collect sufficient data under vacancy conditions. Data collection was done over three weeks, with diverse people count patterns. Users working at their workspaces (or being away from the workspace) accounted for longer time durations of the data collected as would be expected in typical office environments, including short durations of being at (or away from) the workspace or walking to another user for a discussion. At maximum capacity, 4 people were present in the room.

Results of these experiments are shown in Figure 14. From this figure, we see that with probability 0.9, ACE(1) = 0.28, ACE(600) = 0.25, and ACE(9000) = 0.19. When increasing the window, the performance improves due to instantaneous errors being removed as well as temporal filtering.

An example of results from a dataset over a day is shown in Figure 15. The example shows a good estimation of the number of people and also depicts situations where the algorithm results in errors. As we can see, occupancy events that are short in duration (due to situations like having a short coffee break) are not detected at times. We also observe that an overestimation of people count may occur (3 instead of the ground truth 2) - this is likely due to the larger than usual impact of occupancy on temperature.

V. Conclusions and Discussion

We showed that a single-pixel thermopile infrared sensing solution can provide people counting data with high accuracy. We extended the CUSUM-RLS filter by considering temperature change estimation, in turn using this to estimate people count. The proposed approach was shown to achieve an ACE of 0.11 and 0.19 for 90% of instants respectively when considering 15 minute windows for simulated and experimental datasets.

A number of extensions to this work may be explored in future. In the thermopile signal model in (4), we considered

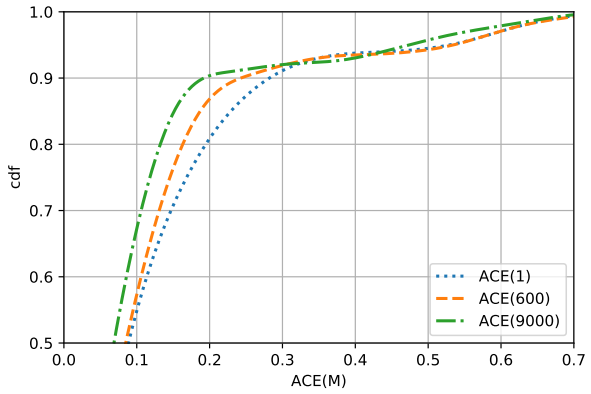

Fig. 14. Cumulative distribution for the results of the real experiment results.

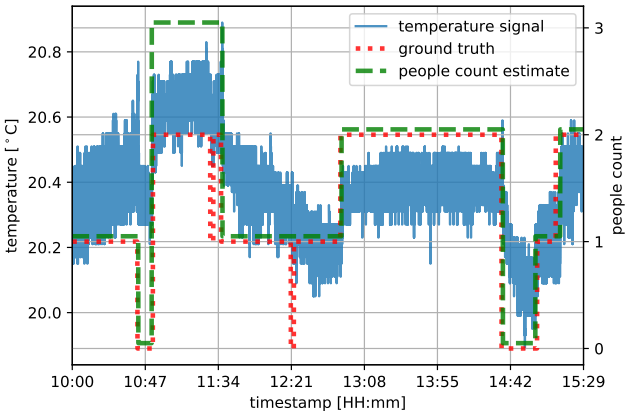

Fig. 15. People count estimation of an experiment dataset.

a memoryless approach to model the influence of the number of people on temperature. This model may be improved by incorporating the memory of the previous state of the number of people before the count changes.

We considered people counting with a thermopile infrared combi-sensor. In an office deployment, a single area (e.g. large meeting room or open office) may have multiple such sensors with partially overlapping FoVs. Estimating people count in such a sensor system would be a topic of further exploration. Extending this work to consider user mobility and alternate sensor deployments are also topics of future study.

REFERENCES

[1] A. Beltran, V. L. Erickson, and A. E. Cerpa, "ThermoSense: Occupancy thermal based sensing for HVAC control," in *Proceedings of the 5th ACM Workshop on Embedded Systems For Energy-Efficient Buildings*, ser. BuildSys'13. New York, NY, USA: Association for Computing Machinery, 2013, p. 1–8.

[2] J. Zhang, R. G. Lutes, G. Liu, and M. R. Brambley, "Energy savings for occupancy-based control (OBC) of variable-air-volume (VAV) systems," Pacific Northwest National Lab (PNNL), Richland, WA (United States), Tech. Rep., 2013.

[3] Z. Yang, A. Ghahramani, and B. Becerik-Gerber, "Building occupancy diversity and HVAC (heating, ventilation, and air conditioning) system energy efficiency," *Energy*, vol. 109, pp. 641 – 649, 2016.

[4] P. Gupta and G. Parija, "Efficient seat utilization in global IT delivery service systems," in *2009 IEEE International Conference on Services Computing*, Sept 2009, pp. 97–103.

[5] R. Pereira, K. Cummiskey, and R. Kincaid, "Office space allocation optimization," in *IEEE Systems and Information Engineering Design Symposium*, April 2010, pp. 112–117.

[6] E. K. Burke, P. Cowling, and J. D. L. Silva, "Hybrid population-based metaheuristic approaches for the space allocation problem," in *Proceedings of the 2001 Congress on Evolutionary Computation (IEEE Cat. No.01TH8546)*, vol. 1, 2001, pp. 232–239 vol. 1.

[7] D. Caicedo and A. Pandharipande, "Location data analytics for space management," in *IEEE World Congress on Services*, June 2017, pp. 1–8.

[8] M. Eldib, N. B. Bo, F. Deboeverie, J. Nino, J. Guan, S. V. de Velde, H. Steendam, H. Aghajan, and W. Philips, "A low resolution multi-camera system for person tracking," in *2014 IEEE International Conference on Image Processing (ICIP)*, Oct 2014, pp. 378–382.

[9] T. Teixeira and A. Savvides, "Lightweight people counting and localizing for easily deployable indoors WSNs," *IEEE Journal of Selected Topics in Signal Processing*, vol. 2, no. 4, pp. 493–502, Aug 2008.

[10] A. B. Chan, Z.-S. J. Liang, and N. Vasconcelos, "Privacy preserving crowd monitoring: Counting people without people models or tracking," in *2008 IEEE Conference on Computer Vision and Pattern Recognition*, June 2008, pp. 1–7.

[11] M. Eldib, F. Deboeverie, W. Philips, and H. Aghajan, "Towards more efficient use of office space," in *Proceedings of the 10th International Conference on Distributed Smart Camera*, ser. ICDSC '16. New York, NY, USA: ACM, 2016, pp. 37–43.

[12] S. Singhal, C. Neustaedter, T. Schiphorst, A. Tang, A. Patra, and R. Pan, "You are being watched: Bystanders' perspective on the use of camera devices in public spaces," in *Proceedings of the 2016 CHI Conference Extended Abstracts on Human Factors in Computing Systems*, ser. CHI EA '16. New York, NY, USA: ACM, 2016, pp. 3197–3203.

[13] K. Wolf, A. Schmidt, A. Bexheti, and M. Langheinrich, "Lifelogging: You're wearing a camera?" *IEEE Pervasive Computing*, vol. 13, no. 3, pp. 8–12, 7 2014.

[14] A. Tyndall, R. Cardell-Oliver, and A. Keating, "Occupancy estimation using a low-pixel count thermal imager," *IEEE Sensors Journal*, vol. 16, no. 10, pp. 3784–3791, May 2016.

[15] J. Tanaka, H. Imamoto, T. Seki, and M. Oba, "Low power wireless human detector utilizing thermopile infrared array sensor," in *SENSORS, 2014 IEEE*, Nov 2014, pp. 462–465.

[16] J. Tanaka, M. Shiozaki, F. Aita, T. Seki, and M. Oba, "Thermopile infrared array sensor for human detector application," in *2014 IEEE 27th International Conference on Micro Electro Mechanical Systems (MEMS)*, Jan 2014, pp. 1213–1216.

[17] M. Kuki, H. Nakajima, N. Tsuchiya, and Y. Hata, "Multi-human locating in real environment by thermal sensor," in *IEEE International Conference on Systems, Man, and Cybernetics*, Oct 2013, pp. 4623–4628.

[18] D. Caicedo and A. Pandharipande, "Distributed illumination control with local sensing and actuation in networked lighting systems," *IEEE Sensors Journal*, pp. 1092–1104, March 2013.

[19] ——, "Distributed ultrasonic zoned presence sensing system," *IEEE Sensors Journal*, vol. 14, no. 1, pp. 234–243, Jan 2014.

[20] S. Depatla, A. Muralidharan, and Y. Mostofi, "Occupancy estimation using only WiFi power measurements," *IEEE Journal on Selected Areas in Communications*, vol. 33, no. 7, pp. 1381–1393, July 2015.

[21] O. T. Ibrahim, W. Gomaa, and M. Youssef, "CrossCount: A deep learning system for device-free human counting using WiFi," *IEEE Sensors Journal*, vol. 19, no. 21, pp. 9921–9928, Nov 2019.

[22] P. M. Djuric, M. Vemula, and M. F. Bugallo, "Target tracking by particle filtering in binary sensor networks," *IEEE Transactions on Signal Processing*, vol. 56, no. 6, pp. 2229–2238, June 2008.

[23] K. Modepalli and L. Parsa, "Dual-purpose offline led driver for illumination and visible light communication," *IEEE Transactions on Industry Applications*, vol. 51, no. 1, pp. 406–419, Jan 2015.

[24] R. B. D'Agostino, "An omnibus test of normality for moderate and large size samples," *Biometrika*, vol. 58, no. 2, pp. 341–348, 1971.

[25] R. B. D'Agostino and E. S. Pearson, "Tests for departure from normality. empirical results for the distributions of b2 and $\sqrt{b1}$," *Biometrika*, vol. 60, no. 3, pp. 613–622, 1973.

[26] Melexis MLX90614 datasheet, https://www.melexis.com/-/media/files/documents/datasheets/mlx90614-datasheet-melexis.pdf, accessed Feb 1, 2020.

[27] F. Gustafsson, *Adaptive Filtering and Change Detection*. Wiley, 2001.

[28] W. Shen, G. Newsham, and B. Gunay, "Leveraging existing occupancy-related data for optimal control of commercial office buildings: A review," *Advanced Engineering Informatics*, vol. 33, pp. 230 – 242, 2017.